

1

2

Journal of Archaeological Science: Reports, Volume 37, June 2021, Article number 102906  
DOI:10.1016/j.jasrep.2021.102906

3

4

5

**Assessing the reliability of microbial bioerosion features in burnt  
bones: A novel approach using feature-labelling in  
histotaphonomical analysis**

7

8

9

10

11

12

13 Authors

14 Emese I. VÉGH<sup>1</sup>, Andrea CZERMAK<sup>1</sup>, Nicholas MÁRQUEZ-GRANT<sup>2</sup> and  
15 Rick J. SCHULTING<sup>1</sup>

16 <sup>1</sup>School of Archaeology, University of Oxford,

17 <sup>2</sup>Cranfield Forensic Institute, Cranfield University, Defence Academy of the  
18 United Kingdom

19 Corresponding Author: Emese I. Végh, [emese.vegh@wolfson.ox.ac.uk](mailto:emese.vegh@wolfson.ox.ac.uk),  
20 Wolfson College, Linton Road, Oxford, OX2 6UD

## 21 Abstract

22 **Objectives:** Recent histotaphonomic studies have focused on the presence of features thought  
23 to be caused either by bacteria (microscopic focal destruction/MFD and cyanobacterial  
24 tunnelling) or fungal (Wedl tunnelling types 1 and 2) attack on unburnt bone. Identifying  
25 these characteristics on burnt bones could indicate the state of decomposition before burning,  
26 with important repercussions for both archaeological and forensic contexts.

27 **Materials and Methods:** Fleshed pig (*Sus scrofa*, N=25) tibiae were left exposed on a field,  
28 then collected at 14-, 34-, 91-, 180-, 365-day intervals before being burnt in an outdoor fire  
29 ( $\leq 750$  °C). Fresh (fleshed) legs (N=10) acted as unburnt and burnt controls. Thin sections  
30 were examined using transmitted light microscopy and backscattered scanning electron  
31 microscopy. Diagenetic traits were quantitatively and systematically assessed by a novel data  
32 labelling application developed for this study.

33 **Results:** Features meeting the published characteristics of microbial bioerosion ('Wedl  
34 tunnelling', 'lamellate' and 'budded MFD') were significantly correlated with time since  
35 deposition on the unburnt bones. The presence of features resembling 'Wedl 2 tunnelling' on  
36 fresh burnt bones indicates that they are an artefact. Only budded MFD increased  
37 significantly over time in the burnt groups. Features meeting the published characteristics of  
38 Wedl 2 tunnelling were present on the fresh burnt bones.

39 **Discussion:** The presence of many features seemingly indistinguishable from those caused by  
40 bioerosion on the freshly burnt control bones suggests that burning is not only able to conceal  
41 features thought to be the result of bioerosion but can produce them as well. Thus, such  
42 features are not a reliable indication of bioerosion. Budded MFD may be a viable indicator  
43 but more research is required.

## 44 Keywords

45 Microbial bioerosion, burning, bone, cremation, taphonomy

46  
47  
48  
49

## 50 Introduction

51

52 Understanding early postmortem changes to the body is of interest in many fields,  
53 including archaeology, physical anthropology, forensic science, palaeobiology, and  
54 palaeontology. Deciphering early bone diagenesis and shedding light on the processes that  
55 lead to fossilisation presents a challenge, one that is further exacerbated when bone is  
56 subjected to cremation. Identifying bioerosion on burnt bones would open the possibility of  
57 establishing whether a body had gone through a decomposition phase with soft tissue still  
58 present prior to burning. This research aims to investigate whether bioerosion features can be  
59 used as an indication of decomposition on burnt bones, which has implications to  
60 understanding funerary practices in the archaeological record as well as understanding the  
61 sequence of events leading to deposition in forensic investigations.

62 Burning of the body can occur either when the body is fully fleshed (e.g. homicide,  
63 suicide, accidental fires, cremation) or once it has decomposed to different degrees (e.g.  
64 burning to conceal evidence of murder, cremation, accidental fires, freeing up space in a  
65 cemetery) in both archaeological and forensic contexts. Early studies mainly focused on  
66 establishing whether bone was at either of the two extremes – fleshed or dry – of the  
67 spectrum when burnt (Baby, 1954; Binford, 1963; Buikstra and Swegle, 1989; Etxeberria,  
68 1994; Spennemann and Colley, 1989; Whyte, 2001). The methods employed were primarily  
69 macroscopic, recording the presence of warping and of thumbnail fractures (Buikstra &  
70 Swegle, 1989; Spennemann & Colley, 1989; Whyte, 2001). However, this has been shown to  
71 be relate primarily to collagen content (Gonçalves et al., 2011). Currently, it remains  
72 challenging to identify the body's state of decomposition before burning.

73 A reliable method of establishing the body's stage of decomposition at the point of  
74 burning would help determine whether this occurred immediately or sometime after death. In  
75 archaeology, the interaction between anthropogenic and natural processes is vital to  
76 understand human behaviour connected to past funerary rites. For example, it has been  
77 suggested that at some Neolithic and Bronze Age sites in Ireland, including the passage  
78 tombs of the Boyne Valley and Fourknocks, as well as Kilgreany cave (Waterman, 1978;  
79 Dowd, 2008; Cooney et al. 2014), human remains were either passively or actively  
80 excarnated before inhumation and cremation. At other Irish sites, such as Tully, the  
81 excavators claimed that the bodies were burnt with full soft tissue coverage (Wells, 1978).  
82 These claims were based on supposedly diagnostic fracture patterns, which, as noted above,  
83 may be problematic.

84           There are a few cases discussed in the forensic anthropological literature in which a  
85 single individual has been found partially burnt (Bontrager and Nawrocki 2008; Garrido-  
86 Varas and Intriago-Leiva 2015). The postmortem intervals were established using both the  
87 signs of carnivore gnawing and patterned thermal destruction. However, usually only  
88 fragmented calcined remains are encountered. Thus, there is a need for better and more  
89 accurate methods of determining the stage of decomposition from a single burnt skeletal  
90 fragment.

91           Bone is a complex, composite material, which undergoes diagenetic alterations post-  
92 deposition. Three distinct diagenetic pathways can be distinguished (Collin et al., 2002): (1)  
93 chemical degradation of the organic component (collagen hydrolysis); (2) chemical  
94 degradation of the inorganic phase (bioapatite dissolution); and (3) microbial degradation of  
95 both phases (Child, 1995; Hedges and Millard, 1995; Millard, 2001; Collins et al., 2002;  
96 Nielsen-Marsh and Hedges, 2002; Huisman et al., 2017; Turner-Walker and Jans, 2008;  
97 Kontopoulos et al., 2016). Pathway 3 presumably happens either (1) rapidly after death as it  
98 is thought to be linked to putrefaction processes involving soft tissues (Huisman et al., 2017;  
99 Collins et al., 2002; Jans, 2005; Fernández-Jalvo et al., 2010) or (2) by soil bacteria post-  
100 deposition (Turner-Walker, 2012, 2019; Kendall et al. 2018). This study focuses on this  
101 pathway's (i.e. microbial degradation) supposedly diagnostic features in an effort to shed  
102 light on the early postmortem history of the remains.

103           Histotaphonomy, the taphonomy of bone at the microstructural level, has been often  
104 employed by researchers to investigate the biological deterioration of bone (e.g. White and  
105 Booth, 2014; Kontopoulos et al., 2016). Many studies use features of bacterial attack on  
106 unburnt bones to inform on the initial postmortem period of the body (Child, 1995; Jans et  
107 al., 2004; Nielsen-Marsh, et al., 2007; Hollund, et al., 2012; Hollund, et al., 2014; White and  
108 Booth, 2014). Whether the origin of the bioerosive bacteria is endogenous or exogenous,  
109 most studies focus on archaeological bone (Jans et al., 2002; Turner-Walker and Jans 2008;  
110 Brönnimann et al., 2018), and some on recent bone (Yoshino, et al., 1991; White and Booth,  
111 2014; Kontopoulos et al., 2016; Lemmers et al., 2020). Furthermore, to our knowledge there  
112 have only been two studies on histotaphonomic features on burnt bones (Grévin et al., 1991;  
113 Lemmers et al., 2020). Grévin et al., (1991) reported that human bones from a Late Bronze  
114 Age site at Pincevent, France, had been buried for weeks to months prior to cremation based  
115 on microradiographs showing 'typical' postmortem bacterial attack. Recently, Lemmers et  
116 al., (2020) proposed that bioerosion features survive in burnt bones and can be readily  
117 distinguished from alterations in the microstructure caused by burning.

118 All scholarship agrees that there is a need for more experimental histological studies.  
 119 This paper aims to assess whether bioerosion features are useful indicators of decomposition  
 120 in burnt bones.

121 1.1 Histotaphonomic features in bone  
 122

123 The specific causative agents of microstructural changes are poorly known, but  
 124 mainly they are attributed to bacteria, fungi, or marine based organisms (Bell, 2012a).  
 125 Microbiological decay of the body commences soon after death. Bacteria and fungi alter hard  
 126 tissues by entering through bone’s vasculature (Bell et al., 1996; Millard, 2001). The bacterial  
 127 flora in the gut initially affect the bone from the endosteal surface, while exogenous bacteria  
 128 from the environment (e.g. soil) attack the bone from the periosteal surface (Hackett, 1981;  
 129 Jans, 2008; Daniel and Chin 2010; Boaks et al., 2014; White and Booth, 2014; Kontopoulos  
 130 et al., 2016).

131 Morphological changes to bone resulting from bioerosion was first described by Wedl  
 132 (1864) and Roux (1887), and subsequently by Hackett (1981) and Garland (1987). These  
 133 changes include (1) small channels (Wedl, 1864) caused by fungi (Roux, 1887), (2)  
 134 microscopic focal destruction (MFD), which can be linear longitudinal, lamellate, or budded  
 135 (Hackett, 1981), and (3) other types of diagenetic changes, such as reduction in birefringence,  
 136 inclusions, and infiltrations (Garland, 1987). Hedges, Millard, and Pike (1995) developed the  
 137 *Oxford Histological Index* (OHI) to approximate the preservation of bone histology. The OHI  
 138 is still used in bone histology studies, providing an ordinal scale assessment of the degree to  
 139 which bone is affected by bioerosion. We build on this here by including a quantitative  
 140 assessment of the percentage of the bone affected.

141 More recent research has focused mainly on the presence of MFD, Wedl tunnelling, Wedl  
 142 type 2, and cyanobacterial tunnelling on unburnt bone (see Table 1).

Feature	Appearance	Causative agent	Context and Environment
Microscopic Focal Destruction (MFD)	Linear, Budded, or Lamellate structures around Haversian canals	Endogenous bacteria (Bell et al., 1996; Jans et al., 2004; Jans, 2013; Nielsen-Marsh et al., 2007; Trueman and Martill, 2002; White and Booth 2014)	Terrestrial
		Soil bacteria (Turner-Walker, 2014; Grine et al., 2015; Kontopoulos et al., 2016; Kendall et al., 2018; Morales et al., 2018)	

Wedl tunnelling	Dendritic structures	Fungi (Hackett, 1981; Bell et al., 1991; Trueman and Martill, 2002)	Marine (Garland, 1987; Millard, 1993)
			Terrestrial: surface exposed and/or buried de-fleshed bones (Trueman and Martill, 2002; Jans, 2008; Brönnimann et al., 2018)
			Oxygenated, wet environments in neutral to acidic soils (Huisman et al., 2009, 2017)
Wedl type 2/Enlarged canaliculi/enlarged osteocyte lacunae/Non-Wedl MFD	Enlarged canaliculi, resembling a spider-like structure	Fungi (Trueman and Martill, 2002; Kontopoulos et al., 2016; Kontopoulos, 2019)	Terrestrial
		Bacteria (White and Booth, 2014; Booth, 2016)	
Cyanobacterial tunnelling	Tunnelling from periosteal surface of bone	Bacteria (Bell et al., 1991; Jans, 2008; Bell, 2012a; Turner-Walker, 2012, Turner-Walker 2014)	Marine- or fresh water (Bell et al., 1991; Jans 2008; Bell, 2012a; Turner-Walker, 2012, Turner-Walker, 2014)

143 *Table 1. Microbial bioerosion features, their thought to be causative agents, contexts and*  
144 *environments in the literature.*



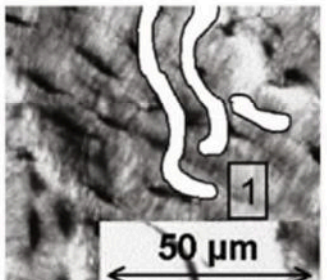
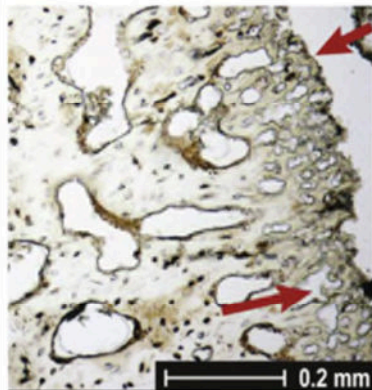

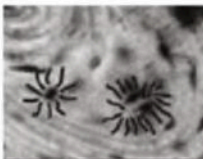
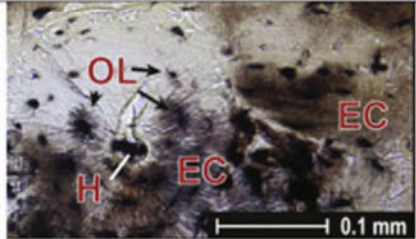

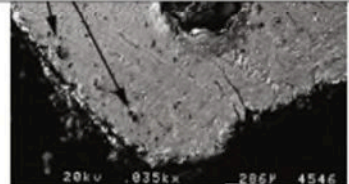
145 Diagenetic features on bones are usually studied under either transmitted light  
146 microscopy (Jans et al., 2002; Jans et al., 2004; Jans 2005; Tjelldén et al., 2018) or electron  
147 microscopy (Bell et al., 1991; Bell, 2012b; Turner-Walker, 2014), with a few studies  
148 employing both methods (Huisman et al., 2017; Turner-Walker 2019). General changes in  
149 bone microstructure due to bacterial attack manifest in demineralised (darker) and adjacent  
150 hypermineralised (brighter) areas on the backscattered scanning electron microscope  
151 (BSEM), which recently has been proposed to be a more effective means of identifying  
152 bioerosion features (Turner-Walker 2019).

153 Complicating discussion of histotaphonomical features is the fact that morphologically  
154 identical or similar features have been given different terms in the literature (see Table 2). For  
155 example, the same dendritic features often called Wedl tunnels (Brönnimann, et al., 2018),  
156 are also called as non-Wedl MFD (Fernández-Jalvo et al., 2010), Wedl type 2 (Trueman and  
157 Martill, 2002; Brönnimann et al., 2018), lichen penetration (Fernández-Jalvo et al., 2010),  
158 and early stage of non-Wedl MFD (White and Booth, 2014). This distinction is crucial, since  
159 for example Wedl tunnelling are thought to be caused by fungi from the burial environment  
160 (Fernández-Jalvo et al., 2010; Brönnimann et al., 2018), while non-Wedl MFD have been

161 attributed to bacterial activity, most often from the gut (Bell et al., 1996; Jans et al., 2004;  
162 Jans, 2013; Nielsen-Marsh et al., 2007; Trueman and Martill, 2002; White and Booth, 2014).  
163 The present study uses the terminology outlined by Brönnimann et al. (2018) because of its  
164 clear illustrations and descriptions.

**Table 2**

Identical histotaphonomic features named differently across the literature.

Feature	Different naming of the features across the literature			
	 <p data-bbox="459 766 851 821">Cyanobacterial tunnelling, (Huisman et al., 2017, 20, Fig 4.A)</p>	 <p data-bbox="918 782 1288 837">Wedl tunnelling (Jans et al., 2004, 89, Fig 1)</p>	 <p data-bbox="1310 893 1680 973">Cyanobacterial tunnelling (Brönnimann et al., 2018, 50, Fig 4G)</p>	 <p data-bbox="1713 893 2004 981">Wedl tunnelling – no scale provided, x170 (Hackett, 1981, 251, Fig 2)</p>
	 <p data-bbox="459 1236 873 1292">Wedl type 2 (Brönnimann et al., 2018, 50, Fig 4E)</p>	 <p data-bbox="918 1268 1288 1388">Expanded osteocytic lacunae and canaliculi due to environmental infiltration (Tjeldén et al. 2018, 412, Fig. 6)</p>	 <p data-bbox="1321 1181 1668 1236">Lichen penetration (Fernández-Jalvo et al., 2010, 74, Fig 7.4)</p>	

169 1.2 Histology of burnt bone

170

171 The primary focus of burnt bone histology studies has been on estimating fire  
 172 temperature and duration (Herrmann, 1976, 1977; Nicholson, 1993; Holden et al., 1995a,b;  
 173 Quatrehomme et al., 1998; Ubelaker, 2009; Absolonova et al., 2013; Imaizumi et al., 2014;  
 174 Cambra-Moo et al., 2017) or on species identification (Cattaneo et al., 1999) using  
 175 histomorphometry or histomorphology (Table 3). There is a considerable disagreement  
 176 between different authors on when, and if, identifiable histological changes take place. The  
 177 histological structure of bone has been variously reported to be nearly identical to that of  
 178 unburnt bone when burnt under 600°C (Bradtmiller and Buikstra, 1984), 700°C (Herrmann,  
 179 1977), 900°C (Squires et al., 2011), or 1200°C (Cattaneo et al., 1999). However, it is  
 180 unknown whether these were bone or air temperatures, which might be a source of  
 181 discrepancy. Other complicating factors include the method of burning (e.g., furnace or  
 182 natural fire), the type, size, and state of the bone, and the presence/absence of soft tissues.

183 Investigating histomorphological changes due to burning are essential to the current  
 184 study, because these can influence the appearance of microbial bioerosion and hence their  
 185 recognition to identify the postmortem stage at which the bones were burnt.

Temperature (°C)	Histomorphometric Changes	Histomorphology Changes
500	Increase in size and number of cracks due to differential shrinkage of bone tissues (Imaizumi et al., 2014)	Cracking, minute fissures, separation of the osteons from interstitial lamellae (Imaizumi et al., 2014)
<600	No change, identical to unburnt bones (Absolonova et al., 2013) No cracking with minimal carbon deposits (Hanson and Cain, 2007) Microfeatures identifiable, but less well preserved (Caroll and Squires, 2020)	
600	Increase in osteon size diameter (Bradtmiller and Buikstra, 1984)	Individual lamellae often indistinguishable (Nelson, 1992) Histological structures disappear with extensive carbon deposits (Hanson and Cain, 2007)
	Haversian canals increased in size while the osteon's diameter decreased (Nelson, 1992)	
<700	No change, identical to unburnt bones (Herrmann, 1976, 1977) Cracks present outwards of vascular canals (Hanson and Cain 2007)	
700-800	Structural changes occur (Herrmann, 1976, 1977; Hummel and Schutkowski, 1987; Absolonova et al., 2013)	
800	No changes below, shrinkage above (Van Vark, 1970)	No major changes below (Van Vark, 1970)
	No significant shrinkage (Cattaneo et al., 1999)	Lamellar structure of bone is lost (Holden et al., 1995b)

900	Microstructural changes occur (Squires et al., 2011)	Haversian and Volkmann's canals cannot be distinguished, no microstructure preserved (Squires et al., 2011) Granular surface appears (Castillo et al., 2013) 700-900 °C: Degeneration of microscopic structures (<60% of area, Carroll and Squires, 2020)
1000	Shrinkage occurs (Cattaneo et al., 1999)	Haversian canals survive, while Volkmann's canals, circumferential lamellae, resorption cavities are hard to differentiate (Absolonova et al., 2013) Few misshapen Haversian canals survive, but 86.3% of sample area show complete fusion of hydroxyapatite (Carroll and Squires, 2020)
1200	Microstructural changes start to occur (Cattaneo et al., 1999)	
1400		Haversian Canals and osteocyte lacunae indistinguishable (Holden et al., 1995b)
1600	All structural features are completely destroyed (Holden et al., 1995b; Fairgrieve, 2008)	

186 *Table 3. Histomorphometric and histomorphology changes of burnt bone in the literature.*

## 187 Materials and Methods

### 188 2.1 Experiment

189 Fleshed *Sus scrofa domesticus* (pig) tibiae were sourced from a local butcher,  
190 euthanised at 18 months. All limbs were kept in a freezer at -18°C until collection. Pigs, in  
191 addition to being easily sourced, have been widely utilised as a substitute for human bodies in  
192 decomposition, fire, and histology studies (Forbes et al., 2005; Lynn and Fairgrieve, 2009;  
193 Thompson and Inglis, 2009; Bonney et al., 2011; Symes et al., 2012; White and Booth 2014;  
194 Kontopoulos et al., 2016). There is an ongoing discussion on how appropriate pigs are as  
195 human analogues (Matuszewski et al. 2020), but they are considered to be reasonable proxies  
196 in many respects, including bone macro- and microstructure, remodelling, mineral  
197 concentration and density, as well as gut microbiota (Turner and Wiltshire, 1999; Forbes et  
198 al., 2005; Pearce et al., 2007; Wilson et al., 2007; Feng and Jasiuk, 2011; Hollund et al.,  
199 2014; White and Booth, 2014; Kontopoulos et al., 2016). Long bones were chosen for the

200 study because of their common use in histological studies, their large cortical bone area, and  
201 their survival rate (Booth and Madgwick, 2016).

202 The pig tibiae (N=25) were left to decay for 14, 34, 91, 180, and 365 days prior to  
203 burning on an outdoor fire. Fresh fleshed bones (N=10) served as unburnt and burnt control  
204 samples. The first round of fleshed tibiae were sub-aerially deposited on an open grassland  
205 area at Wytham Woods, Oxfordshire, England, in June 2018 and between February and June  
206 2019. The exposed tibiae were protected from scavengers with a cage covered by layers of  
207 iron mesh. Scavenging produced tooth marks on nearly all bones, but only a few bones were  
208 completely removed from the cage (one of the 180-day and four of the 365-day postmortem  
209 bones).

210 Wytham Woods is located in a temperate climate with moderate to high rainfall  
211 averaging 717 mm, with monthly mean temperatures ranging from 1.6 °C in January to 20.3  
212 °C in July with a long-term annual mean of 10.0 °C (Taylor et al., 2011). At collection bones  
213 were partially covered by the soil, which may have instigated exogenous bioerosion. Soil pH  
214 range from 3 to 7 (Taylor et al., 2011).



215

216

217

218

*Fig. 1. Burning of the 14- and 34-day postmortem bones on the pyre. Upper image was taken subsequently after the ignition of the fire, while the lower was taken when the bones have calcined. All outdoor fires were executed in the same manner. The pyres were*

219 *built on a flat clearing, using bricks to provide support for a wire mesh holding the bones, as*  
220 *well as partial protection from the wind. While offering less control over temperature rather*  
221 *than a furnace, the use of an outdoor fire better reflects real-world conditions due to the*  
222 *more variable temperatures of the fire, and the influence of the wind. Each fire was built and*  
223 *maintained in the same manner, using a mixture of hard and soft woods as fuel.*

224

225 Pyres were built and maintained in the same manner (Fig. 1), each fire lasting 2.5-3  
226 hours, until the bones calcined (Fig. 1). Bone temperatures were monitored by a  
227 thermocouple, averaging 553 °C, with a recorded maximum of 751 °C. Maximum fire  
228 temperatures reached 995 °C. The bones were left to cool and subsequently collected for  
229 transport.

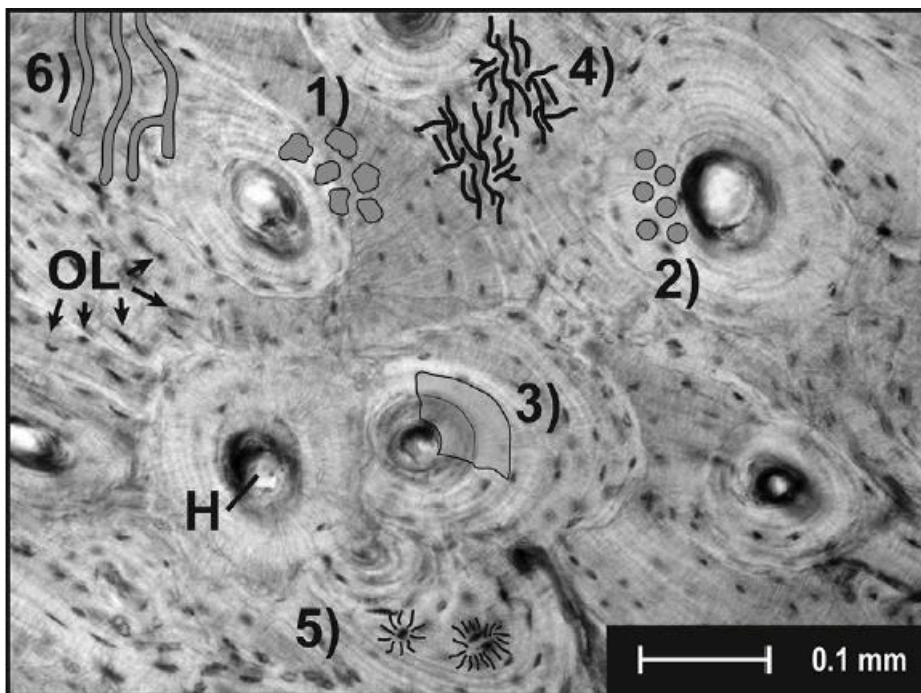
## 230 2.2 Analysis

231

232 Unburnt samples were defatted in a 2:1 chloroform:methanol mixture for between 8  
233 and 20 weeks, in order to remove fat infilling the pores of bone tissues. Samples were taken  
234 before and after burning from the minimum diameter of the tibiae diaphyses. Samples were  
235 embedded undecalcified in transparent epoxy cold mounting resin and a catalyst  
236 (Spectrographic Ltd., Leeds, UK), in order to impregnate the bones within a solid medium to  
237 facilitate sectioning for microscopical analysis (Garland, 1987). The resin blocks (N=56)  
238 were then placed into a desiccator with vacuum pump to inhibit bubble formation. Two  
239 transverse thin sections (~50-70 µm) were cut from each sample using a Buehler saw fitted  
240 with a diamond blade (Buehler, Lake Bluff, IL, USA) and subsequently fixed onto glass  
241 slides using Eukitt mounting medium (Merck, Darmstadt, Germany) and covered with  
242 microscope glass slides.

243 The slides were examined under a Leica DM 2500 P transmission light microscopy  
244 with (Leica, Wetzlar, Germany) using normal and polarised light at 50x, 100x, and 400x  
245 magnification. Each sample was composed of three to five images, which were taken across  
246 the bone with a USB camera (Brunel Microscopes Ltd., Chippenham, UK) per thin section at  
247 50x magnification to represent bone from the periosteal to the endosteal surfaces, through the  
248 mid-cortical region for quantitative analysis. Higher magnification images were taken to  
249 observe and document more closely the features of interest.

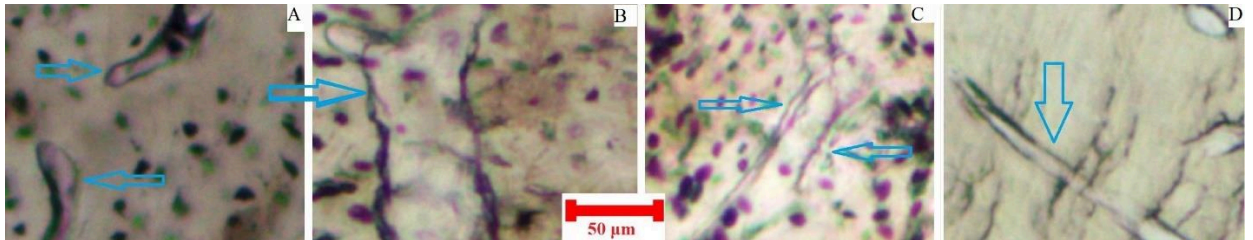
250 Diagenetic traits on the optical microscopy images (N=270) were quantitatively  
251 assessed by calculating the percentage of areas affected by diagenetic and/or heat-induced  
252 features. This was done by a human observer clicking on the features present on each block  
253 (N=27,000) of randomly selected images in a data labelling application built for this study in  
254 Python (Flask web framework) and Javascript (jQuery library) programming languages. Each  
255 image (at 50x magnification) was divided into 100 equal blocks. The random selection of  
256 images across all samples by the application excluded bias in labelling, hence the samples  
257 were examined 'blind'. Results were automatically saved into a database recording whether a  
258 feature was present or absent within a block. The cumulative score of the 100 blocks  
259 estimates the proportion of the initial image that contains a given feature. Features (Fig 2)  
260 were labelled according to descriptions in Brönnimann et al. (2018, 46, Fig. 1), which are in  
261 turn based on figures in Jans (2004, 89, Fig. 1) and Hackett (1981, 250, Fig. 1). Features were  
262 initially labelled according to their closest comparanda in the literature, with no  
263 presuppositions being made regarding the veracity of the labels. This usage is indicated by  
264 single quotation marks. Some features were more variable in appearance than those discussed  
265 in the literature. For example, the label 'cyanobacterial tunnelling' was applied when the  
266 tunnels looked the most like the image in Brönnimann et al. (2018) taking into account tunnel  
267 diameters (Fig. 3) after re-examination of all images by the same researcher (EIV).



268

269 *Fig. 2. Criteria for labelling microbial bioerosion from Brönnimann et al., 2018. 1)*  
270 *Budded MFD; 2) Linear longitudinal MFD; 3) Lamellate MFD; 4) Wedl tunnelling; 5) Wedl*

271 2; 6) Cyanobacterial tunnelling (Brönnimann et al., 2018, 46, Fig. 4). Features that  
272 appeared to be similar to linear MFD were not labelled in this study, because they were  
273 caused by burning.  
274



276  
277 *Fig. 3. Variation of features appearing to be tunnels in the different samples. A and B*  
278 *are of Volkmann's canals, C and D are unidentified channels and hence were labelled having*  
279 *the appearance of features consistent with 'cyanobacterial tunnelling', even though there is*  
280 *no clear indication of cyanobacteria being present in a terrestrial context, and the tunnel in*  
281 *D appears to be connected to a Haversian canal. The features are indicated by the blue*  
282 *arrows. Note the differences in the width of the tunnels. In the literature, maximum tunnel*  
283 *diameters caused by microorganisms have been reported to be between 0.1 and 2.0 micron*  
284 *(terrestrial), 7-18 microns (freshwater), and 5-19 microns (marine, Pesquero et al., 2018).*  
285 *Here, diameters under 20 microns were considered to be 'cyanobacterial tunnelling', while*  
286 *>20 microns were classed as Volkmann's canals. (Transmitted light microscopy, 50x, from*  
287 *left to right: WSF2D2W5\_unburnt, WSF2D2W5\_burnt, WSF1D1M2\_unburnt,*  
288 *WSF1D1M2\_burnt).*

289 The prevalence of features on unburnt and burnt bones was then statistically analysed  
290 using Jupyter notebook in Python programming language (Pandas, Matplotlib, Seaborn,  
291 SciPy, and Numpy libraries). Linear regression was used to measure the strength of the  
292 relationship between the presence (in percentage) of each taphonomic feature and the length  
293 of the postmortem period before and after burning, with statistical significance assessed by  
294 associated p-values ( $\alpha = 0.05$ ). The null hypothesis was that the presence (in %) of a given  
295 feature per bone does not increase with the postmortem interval. The coefficient of variation  
296 (CV) was used to assess the dispersion of the features in different decompositional stages and  
297 burning status.

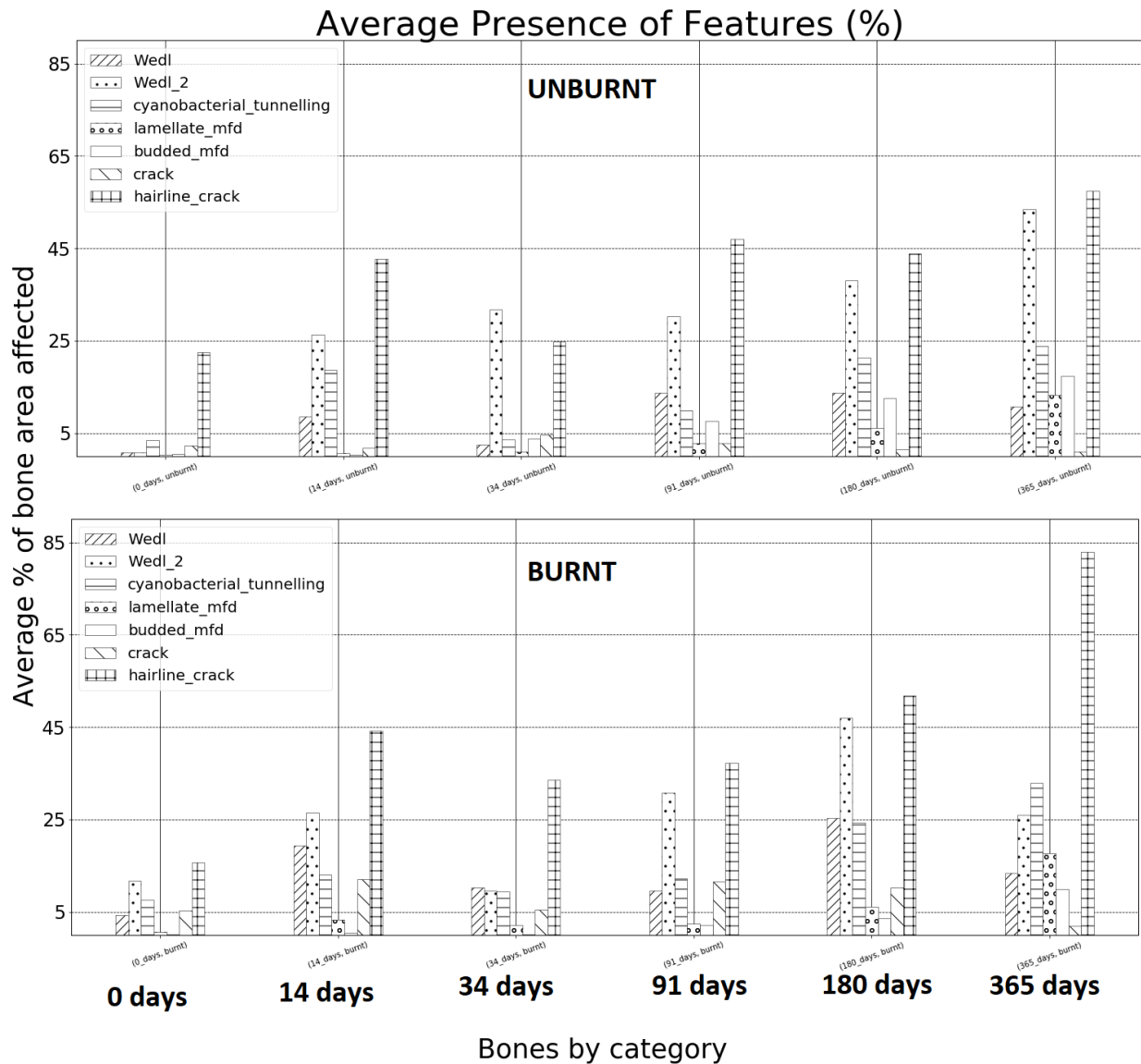
298 Validation of whether or not features were due to bioerosion was then undertaken  
299 using a BSEM detector in the electron microprobe. The contrast on the images resulting from  
300 demineralised and hypermineralised areas can be used to identify bioerosion (Turner-Walker,  
301 2019). The resin blocks were ground with carborundum paper of progressively finer grit size  
302 (800, 1200, 2500). The blocks were then polished on a Buehler wheel and a satin woven  
303 acetate polishing cloth (DP-Dac, Struers A/S) using 3 µm and 1 µm monocrystalline  
304 diamond paste and suspension (DP-Paste M, Struers A/S and MetaDi, Buehler, respectively)  
305 for 30 and 5 minutes, respectively. The mounts were cleaned in an ultra-sonic bath in  
306 petroleum ether (40°-60°C). Samples were carbon-coated using a carbon evaporation coater  
307 (HHV Auto 360), the carbon acting as a conductive layer to prevent charging.

## 308 Results

309

310 The percentage of given features present for each decompositional stage before and  
311 after burning is shown in Fig. 3. The most common taphonomic features affecting the largest  
312 percentage of the bone areas were hairline cracks and those similar to what has been  
313 described in the literature as ‘Wedl type 2’. The latter feature was absent from the unburnt  
314 fresh/control group but was present on the freshly burnt controls. ‘Wedl 2’ was also present  
315 after only 2 weeks of deposition on both the unburnt (26.32%) and burnt (26.43%) groups.  
316 After 1 year, this feature was present on over half of the areas investigated (53.5%).

317 The unburnt control group presented a very small number of ‘Wedl tunnelling’  
318 (0.75%), ‘Wedl 2’ (0.75%), ‘lamellate’ (0.25%) and ‘budded MFD’ (0.50%) and tunnels  
319 resembling ‘cyanobacterial tunnelling’ (3.5%). These are attributed to human labelling errors,  
320 and quantify labelling error, which is negligible for almost all categories, due to the  
321 impossibility of bioerosion being present on the control bones. As cyanobacterial tunnelling  
322 cannot be present on these bones, they are almost certainly mislabelled Volkmann’s canals.  
323 Hairline cracks are abundant on this group (22.5%). This group should not show any sign of  
324 microbial bioerosion, since the pigs were dismembered shortly after death and were not  
325 exposed to soil. Conversely, the burnt fresh/control group exhibited significantly higher  
326 percentages of features consistence with ‘Wedl tunnelling’ (4.25%), ‘Wedl 2’ (11.68%) and  
327 tunnels resembling ‘cyanobacterial tunnelling’ (7.56%) as identified in the literature.



328

329 *Fig. 4. The average presence of the taphonomic features at each stage of*  
 330 *decomposition before (upper) and after (lower) burning.*

331 Diagenetic features increase for all bone categories after burning in all  
 332 decompositional stages. There was a moderate positive linear correlation between time  
 333 passed since deposition and percentage of the presence of ‘Wedl tunnelling’ ( $r=0.442$ ,  
 334  $p<0.0001$ ), ‘lamellate MFD’ ( $r=0.493$ ,  $p<0.001$ ), ‘budded MFD’ ( $r=0.531$ ,  $p<0.001$ ) on the  
 335 unburnt bones, while hairline cracks ( $r=0.278$ ,  $p<0.017$ ), showed a weaker correlation with  
 336 time, though it remained significant (Table 4). Weak but significant correlations were  
 337 observed for ‘Wedl 2’ ( $r=0.254$ ,  $p<0.012$ ) and ‘budded MFD’ ( $r=0.296$ ,  $p<0.006$ ) in burnt  
 338 bones.

Feature	r	p	r	p
	unburnt	unburnt	burnt	burnt
Wedl tunnelling	0.442	0.00009**	-0.016	0.886
Wedl 2	0.170	0.151	0.254	0.012**
Cyanobacterial tunnelling	-0.204	0.084	0.114	0.312
Lamellate mfd	0.493	0.00001**	0.091	0.412
Budded mfd	0.531	0.000001**	0.296	0.006**
Crack	0.064	0.591	0.184	0.095
Hairline crack	0.278	0.017**	0.159	0.150

339 *Table 4. Correlation Coefficient ('r') and p-value ('p') for each analysed feature on the*  
340 *unburnt and burnt bones. H<sub>0</sub>= Presence (in %) of X feature per bone does not increase with*  
341 *postmortem time period. \*\* indicates significant p-values.*

342 The coefficient of variation (CV) shows that hairline cracks had the lowest variability  
343 between samples of the same decompositional stage (Table 5), while 'lamellate' and 'budded  
344 MFD' showed the greatest variability. In general, features were less variable pre-burning than  
345 post-burning. The 91 days unburnt, 180 and 365 days postmortem unburnt and burnt bones  
346 had the lowest CV scores across all features. The 14-day burnt bones with features recalling  
347 'budded MFD' (2.73) showed the highest variability.

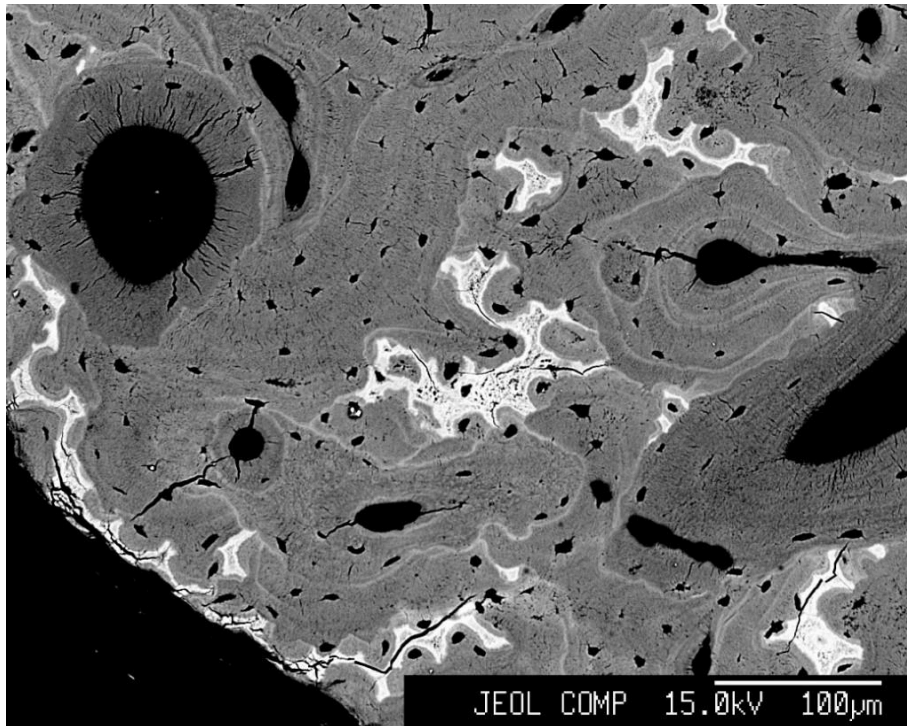
Coefficient of Variation (CV)								
Bones		Wedl	Wedl_2	Cyanobacterial tunnelling	Lamellate MFD	Budded MFD	Cracks	Hairline cracks
0 days	unburnt	1.27	0.66	0.82	2.00	1.15	0.75	0.50
	burnt	1.37	1.71	1.00	1.83	2.73	0.89	1.18
14 days	unburnt	0.72	0.52	0.56	1.36	2.07	1.82	0.30
	burnt	1.15	0.94	0.63	1.00	4.00	0.68	0.61
34 days	unburnt	1.24	0.64	0.73	1.10	1.33	0.94	0.60
	burnt	0.80	1.05	0.71	1.73	2.07	0.74	0.57
91 days	unburnt	0.49	0.70	0.60	0.95	0.98	1.20	0.24
	burnt	1.22	0.94	1.16	1.37	2.21	1.10	0.78
180 days	unburnt	0.43	0.64	0.40	0.55	0.67	1.40	0.31
	burnt	0.93	0.35	0.45	0.87	0.60	0.79	0.45
365 days	unburnt	0.80	0.51	0.36	0.25	0.50	2.00	0.27
	burnt	0.60	0.78	0.50	0.11	0.26	1.00	0.02

348 *Table. 5. Coefficients of variation for each feature on the grouped samples by postmortem*  
 349 *period and state of burning.*

350 The BSEM images (Table 6) present bioerosion-like hypermineralised ‘tunnels’,  
 351 which are due to heavy mineral loading in growing individuals (Fig. 5), and thus not the  
 352 result of bioerosion. A small number of images indicate initial stages of bacterial attack on  
 353 some of the exposed unburnt bones, for instance one of the 3-months exposed unburnt bones  
 354 (Fig. 6). Bioerosion was not present on any of the burnt samples. Generally, contrast varied  
 355 across the burnt bones, while there was no significant difference across the unburnt bones.

<b>Decompositional stage</b>	<b>State</b>	<b>Contrast difference present? (trabecular, mid-cortical, periosteal)</b>	<b>Tunnels/cracks with hypermineralised rims?</b>
Fresh	unburnt	No	No
Fresh	burnt	Yes	No
2 weeks	unburnt	No	No
2 weeks	burnt	Yes	Not generally, except 1
1 month	unburnt	No	Yes
1 month	burnt	No	No
3 months	unburnt	No	Yes, around tunnels/cracks and Wedl 2/MFD
3 months	burnt	Yes	No
6 months	unburnt	No	No
6 months	burnt	Yes	No
12 months	unburnt	No	No
12 months	burnt	Yes	No, but grey colour around tunnels

356 *Table 6. Analysis of compositional images.*



357

358

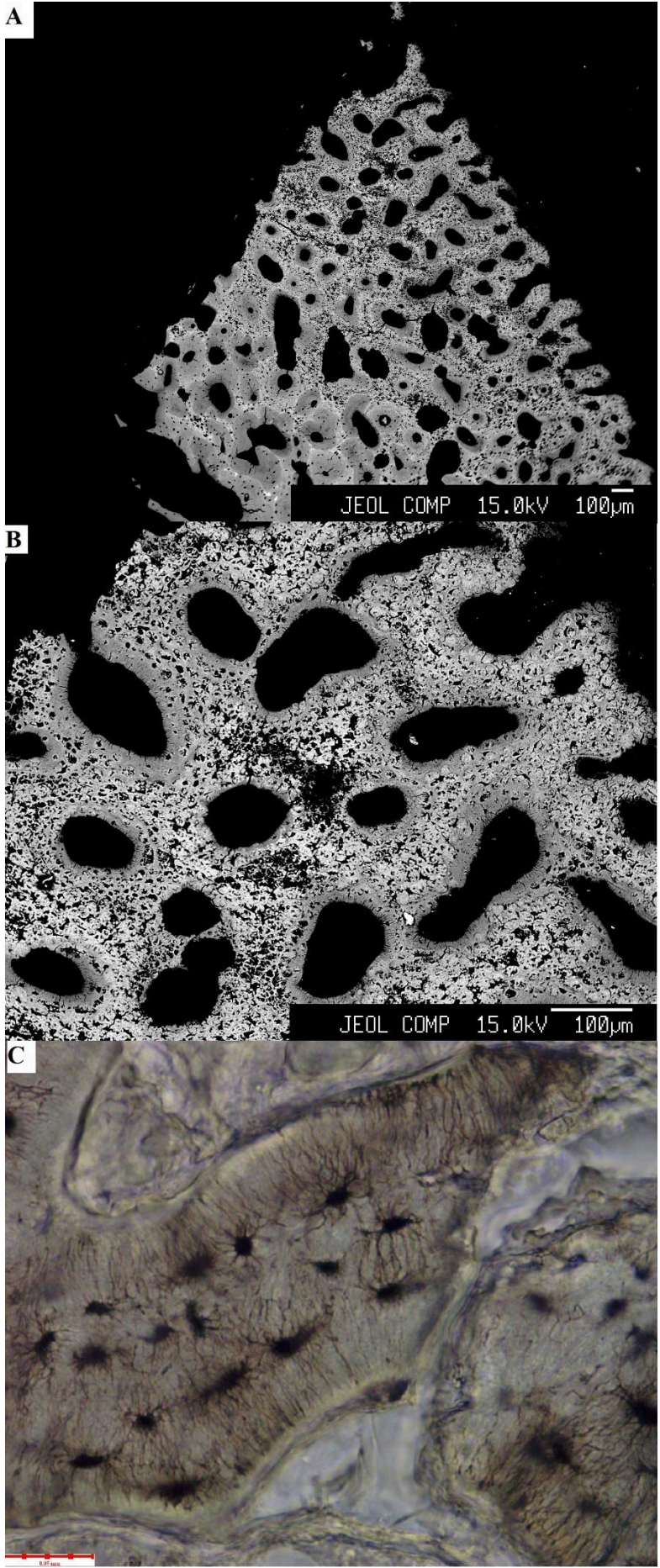
359

360

361

362

*Fig. 5. Backscattered electron image of one of the 1-month postmortem unburnt bones (WSF5D1M3\_unburnt). Note the brighter (hypermineralised) areas around the black (demineralised) 'tunnels' toward the lower end of the image. These bright areas are in fact not due to bioerosion, but to heavy mineral loading in growing individuals where osteonal bone has not replaced the primary lamellar bone.*

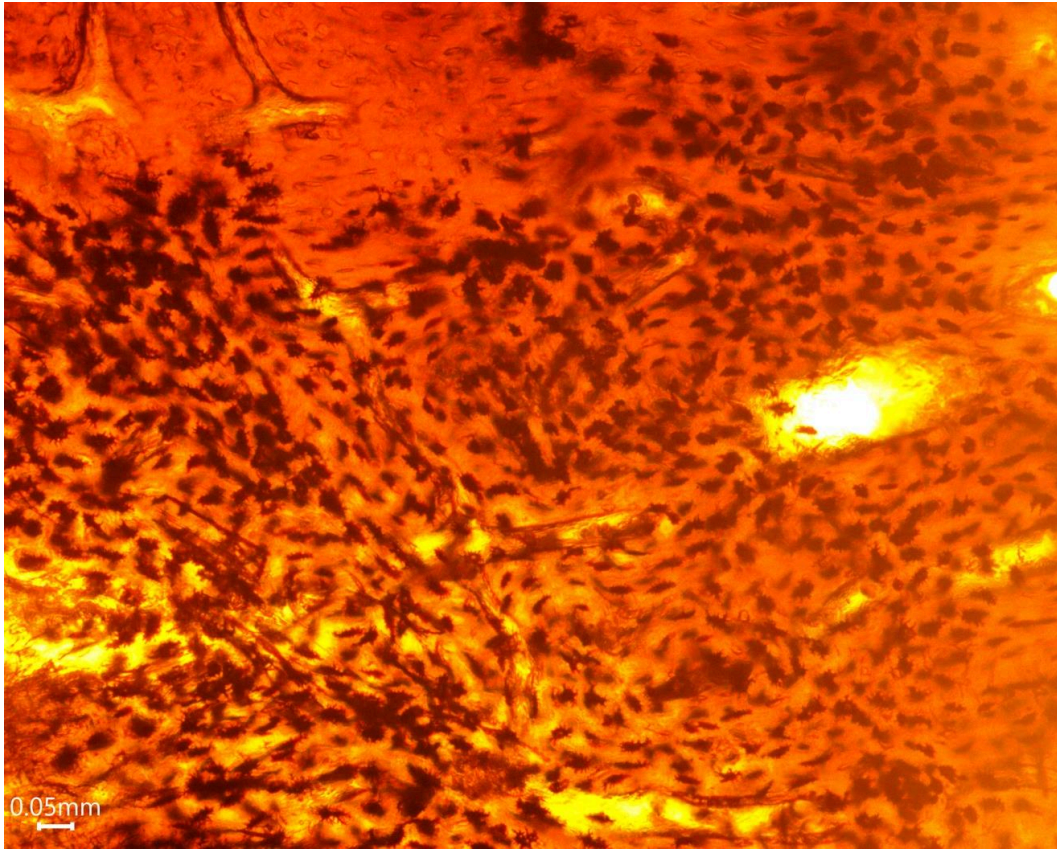


364 *Fig. 6A and B: Backscattered electron image of 3-month postmortem unburnt bone*  
365 *(WSF3D3M3\_unburnt). Note the accumulation of darker (demineralised) circular areas*  
366 *(appearing to be 'Wedl 2' or enlarged canaliculi, but probably naturally demineralised*  
367 *primary bone with microcracks) with bright (hypermineralised) areas around. C:*  
368 *Transmitted light microscopy image of a thin section from the same sample*  
369 *(WSF3D3M3\_unburnt) at 400x magnification.*

370

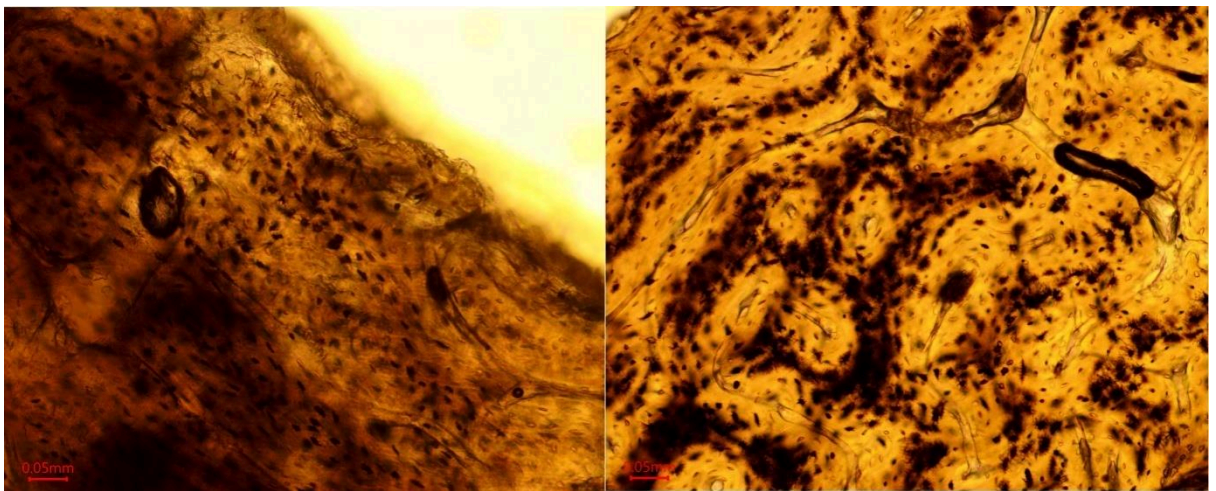
## 371 Discussion

372 Three features associated in the literature with microbial bioerosion are present on the  
373 burnt fresh/control group but absent on the fresh unburnt group. The clear implication is that,  
374 despite their apparent similarity, these are not bioerosional features but are instead artefacts  
375 induced by burning. The feature labelled as 'Wedl type 2' appears on 11.68% of the areas  
376 affected on the burnt fresh/control bones (Fig. 7). The frequency of 'Wedl 2' shows a  
377 statistically significant relationship with postmortem time interval only in the burnt samples.  
378 This feature has been alternatively interpreted as an indication of bioerosion caused by fungi  
379 (Trueman and Martill, 2002), but the aetiology of enlarged lacunae and canaliculi is uncertain  
380 and has also been associated with staining, mineral infiltration, and burning (White and  
381 Booth, 2014; Hanson and Cain 2017). Supporting this, it was found there that these are in fact  
382 carbonised osteocyte cells trapped in the canaliculi due to burning (Fig 8.). This observation  
383 challenges the interpretation of the cremated remains reported by Grévin et al. (1991), where  
384 researchers noted these enlarged canaliculi (referred to here as 'Wedl 2') to be the sign of a  
385 delay of weeks to months before cremation. The high variance (CV=1.71) of 'Wedl 2'  
386 presence on the freshly burnt samples further suggests that the feature was produced by fire.



387

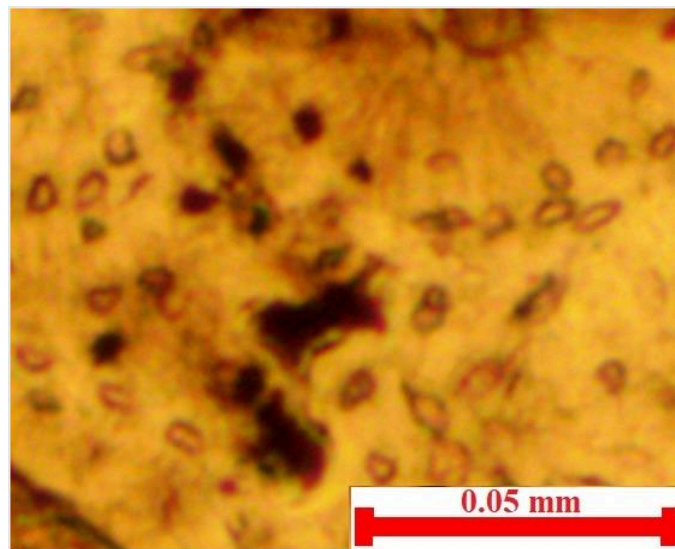
388 *Fig. 7. Staining of the osteocyte-canalicular network that appears to be Wedl type 2*  
389 *on one of the fresh burnt control bones (SWF1FR2\_burnt\_1). The tunnels were labelled*  
390 *'blind' as 'cyanobacterial tunnelling', but these are Volkmann's canals. Neither of these*  
391 *features should be present on freshly burnt bones. Transmission light microscopy, 100x*  
392 *magnification.*



393

394 *Fig. 8. Staining that appears to be 'Wedl 2'. While it is restricted to some canaliculi*  
395 *on the unburnt 6-months postmortem section (left), it affects all osteons on the same burnt*

396 *bone (right). 'Wedl type 2' features are probably due to discolouration on the freshly burnt*  
397 *bones. The source of discolouration can be: (1) sooting from combustion gasses infiltrating*  
398 *the osteocyte-canalicular network after most of the organic matter has burnt out; or (2) iron,*  
399 *manganese, or other metal ions infiltrating the osteocyte-canalicular network prior to*  
400 *burning and then reduced to darker species, such as manganese dioxide or magnetite, when*  
401 *the bones were burnt. While the pig tibiae were not buried, those that were exposed for*  
402 *sufficiently long did become partly covered in soil, which may have presented the opportunity*  
403 *for the infiltration of metal ions. (Sample WSF5D6M1\_1, transmission light microscopy,*  
404 *100x magnification).*



405

406 *Fig. 9. Features resembling 'budded MFD' from a 6-months postmortem burnt bone*  
407 *(WSF5D6M3\_burnt). Transmitted light microscopy, 50x*

408 The frequency of features labelled as 'Wedl tunnelling', and 'lamellate MFD' increase  
409 significantly with decay time on unburnt bones, and although they were present, they showed  
410 no correlation with time since deposition in the burnt groups. Wedl tunnelling is thought to be  
411 attributed to surface exposed and/or buried de-fleshed bones from terrestrial environments  
412 (Trueman and Martill, 2002; Jans, 2008; Brönnimann et al., 2018) and should only happen in  
413 oxygenated wet environments in neutral to acidic soils (Huisman et al., 2009, 2017). Most  
414 bones were covered by soft tissue to different degrees. Less soft tissue coverage means bone  
415 desiccation begins earlier, which might limit the intensity of bioerosion (Jans et al., 2004;  
416 Nielsen-Marsh et al., 2007). Although the 1-month postmortem unburnt bones were much  
417 less affected by 'Wedl tunnelling', the other groups with soft tissues were more affected by

418 this feature. Therefore, no difference was found in bones with remnants of soft tissues and  
419 de-fleshed (by scavenging) bones in the mean bone areas affected by ‘Wedl tunnelling’. Sub-  
420 aerial exposure, the water-logged soil, and the pH (3-7; Farmer, 1995) suggest Wedl  
421 tunnelling should be present (Huisman et al., 2009, 2017), but the fact that it was more  
422 frequent in the burnt than in the unburnt bones suggests that similar features are not due to  
423 fungal activity and can be produced by burning.

424 Although the literature suggests that MFD might indicate an endogenous source of  
425 bacteria, here it can be ruled out. ‘Budded MFD’ was the only feature to consistently show a  
426 statistically significant correlation with time since deposition for both the unburnt and burnt  
427 groups. Post-burning this relationship becomes less robust, suggesting that these features are  
428 more likely to be lost or at least become less visible through burning. In addition, this was the  
429 least reliably present on all bones, followed by ‘lamellate MFD’. ‘Budded MFD’ (Fig. 9)  
430 appeared on the unburnt bones after just 34 days, but it was rarely observed on the same burnt  
431 group (0.19%), increasing slightly in the 3-month postmortem group (2.14%). Its presence  
432 reaches 10% after a year of decomposition post-burning, suggesting that ‘budded MFD’ can  
433 also be produced by burning.

434 If bone colonization by microorganism occurs and manifests as budded MFD, it must  
435 happen before burning, because this destroys the organic component on which bacteria feed  
436 (Grévin et al., 1991). The seasonality of functional activity of microbial communities  
437 associated with putrefaction has been investigated (Pechal et al., 2013). It was noted that the  
438 carbon consumption of bacterial communities in bone was the highest in Spring, when the 1-  
439 and 3-month postmortem bones were placed in the cage. The appearance of budded MFD  
440 after just 1-month postmortem would conventionally be attributed to endogenous bacteria  
441 that spread through the bone’s vasculature causing bioerosion; however, since the pigs were  
442 dismembered shortly after death and frozen until they were deposited in the cages,  
443 endogenous bacteria as a source can be excluded. Although time is thought to be the least  
444 important factor in bioerosion (Piepenbrink, 1986; Piepenbrink and Schutkowski, 1987; Bell  
445 et al., 1996), it is likely that soil bacteria attacks bone over a longer timescale when bones are  
446 buried, especially given that organics (i.e., collagen) can survive for millennia. It has been  
447 shown that microbial extracellular enzyme activity for carbon cycling enzymes significantly  
448 increases in soil closer to the surface (Upton et al., 2019). Thus, the pig legs in this  
449 experiment, lying on and partially submerged in the soil, were arguably exposed to more soil

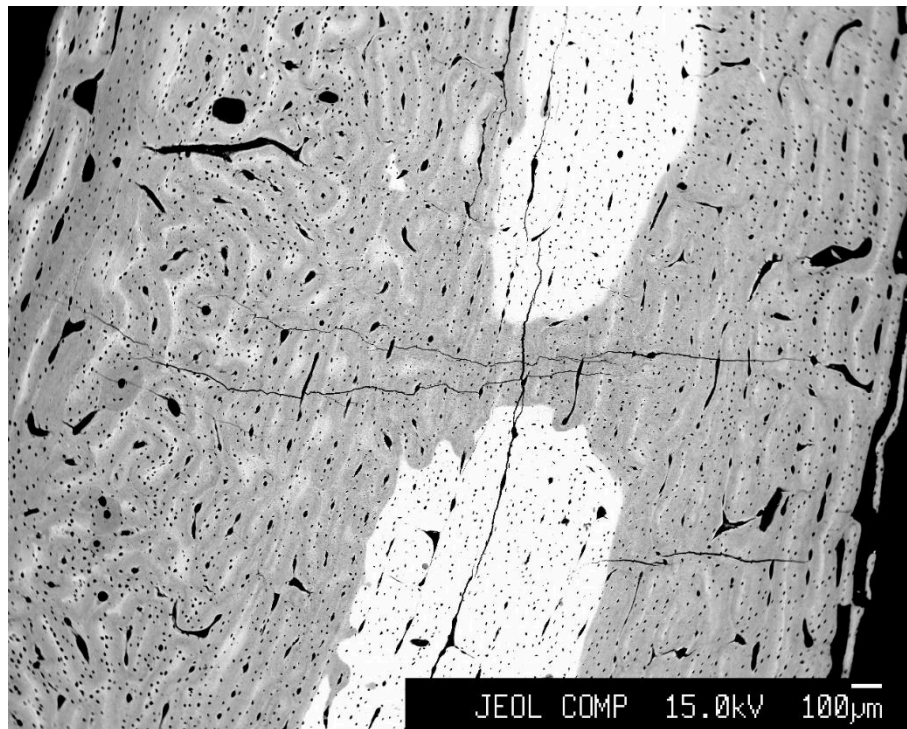
450 microorganisms than if they would have been buried. Although the types of soil bacteria are  
451 environment-specific such that the bioerosion features might manifest differently at various  
452 locations, a large-scale study carried out by Brönnimann et al. (2018) did not find any  
453 relationship between sediment type and intensity of microbial bioerosion.

454 Previous studies found that the first microscopic changes due to burning appear at  
455 varying temperatures ranging from 600-1200°C. It is unknown where these temperatures  
456 were measured (bone or air in furnace). In this study maximum mean bone temperatures  
457 reached  $\leq 750^{\circ}\text{C}$ , while fire temperatures were as high as  $995^{\circ}\text{C}$ . If burnt and unburnt bone  
458 microstructure is indeed indistinguishable at these temperatures, it is possible that these  
459 subtle microscopic changes (e.g. ‘Wedl 2’ and ‘MFD’) caused by burning are mistaken for  
460 bioerosion features. In general, the presence/absence of features on unburnt bones was less  
461 variable than on burnt bones, meaning not all the bones are affected the same way by fire.  
462 Variations might be due to the movement of the wind, flame height, soft tissue coverage, and  
463 this variation might not be present when bones are burnt in a furnace. Thus, it is argued here  
464 that experiments conducted on an outdoor fire give a better indication of real-life conditions  
465 in both forensic and archaeological cases than bones burnt in a furnace.

466 Squires et al. (2011) noted that bones cremated at temperatures between  $600\text{-}900^{\circ}\text{C}$   
467 should have very few, if any, Volkmann’s canals surviving. Conversely, it is argued here that  
468 Volkmann’s canals do survive ‘intense cremation’, as they were observed on all burnt bones.  
469 They were recorded on 3.5% of fresh, unburnt samples, giving an indication of their expected  
470 frequency. The fact that the bones were deposited in a terrestrial context – and hence not  
471 exposed to cyanobacteria – further suggests that these features are mostly Volkmann’s canals,  
472 which can assume a variety of forms depending on the angles at which the bone is sectioned,  
473 and so may be responsible for this discrepancy.

474 Hairline cracks are most probably due to the contraction and expansion of bone  
475 attributable to weather changes, explaining the feature’s positive correlation with longer  
476 decay times in the unburnt groups, which disappeared post-burning. Cracks are considered to  
477 be indications of collagen degradation (Huisman et al., 2017), but no statistically significant  
478 increase was observed with time of deposition. Neither feature appears to be a useful  
479 indicator for degradation in the bones, not least because the preparation of thin sections  
480 and/or burning can cause them. The black enlarged lacunae and canaliculi may be present  
481 because of carbon incorporation into the uneven surfaces of bone.

482 Demineralised and hypermineralised foci were sometimes present on the BSEM  
483 images of the unburnt bones. However, these foci did not resemble tunnels on BSEM images  
484 published by Fernández-Jalvo et al. (2010) and Turner-Walker (2019). Bright, heavily  
485 mineralised areas on the unburnt bones (e.g. Fig. 5) may instead relate to the structure of  
486 bone in young individuals, in which osteonal bone has not yet replaced the primary lamellar  
487 bone, producing a mixture of darker, less dense (younger) and heavier mineralised (older)  
488 areas (Boskey and Coleman, 2010), which can be mistaken for tunnelling. Hypermineralised  
489 areas with a less diffused degradation pattern than has been previously documented (Turner-  
490 Walker and Syversen 2002; Turner-Walker and Peacock 2008) suggest early bacterial  
491 bioerosion in some of the 3-months postmortem unburnt bones. All bioerosion-like features  
492 were obliterated through the burning process (Fig. 10). Therefore, BSEM is not a useful  
493 technique for identification of bioerosion features on burnt bones.



494

495 *Fig. 10. Contrast differences due to burning of a 6-month decayed bone sample*  
496 *(WSF5D6M1\_burnt). Note the central mineralised areas. (Electron microprobe, backscatter*  
497 *electron detector image.)*

498 This study was conducted simultaneously with another recent study by Lemmers et al.  
499 (2020), with similar overall aims and methods. Although they suggest that bioerosion lesions  
500 have the potential to act as a proxy for the pre-burnt condition of the body, the opposite is

501 suggested here. The cause of this discrepancy might be that in the current study fresh, fleshed  
502 tibiae were burnt as controls, while the freshest bones in Lemmers et al.'s (2020) study were  
503 >3 years postmortem and may have been embalmed with a decomposition accelerator  
504 compound. In our study features indistinguishable from bioerosional features as described in  
505 the literature appeared on the fresh burnt controls, suggesting that they were produced by  
506 burning.

507         Limitations of the present study include the use of pigs as a proxy for humans and  
508 their young age (18 months), which might make them more susceptible to bioerosion due to  
509 the higher amount of organic matter in the bones. The data from the 1-year postmortem group  
510 are based on two samples, because the rest were removed by scavengers during the exposure  
511 phase. It was not possible to get access to a microtome, so thin sections were cut with a  
512 Buehler saw, producing a less consistent thickness across samples. All labelling was executed  
513 by one researcher (EIV) and due to the sheer number of blocks (N=27,000) some may have  
514 been incorrectly labelled. Balanced against this is the consistency in approach to  
515 identification that this permitted. Finally, the bones were not exposed to endogenous  
516 bioerosion, which should be the focus of future studies.

## 517 Conclusions

518

519         This study aimed to establish the utility of diagenetic features as a proxy for the body's  
520 state of decomposition prior to incineration. Ours is the first histotaphonomic study to apply a  
521 data labelling application, built for this purpose, to statistically assess bioerosion. We  
522 highlight the inconsistency in the literature concerning the naming of diagenetic features and  
523 their considered aetiologies. Although most recent literature is concerned with what the  
524 source of bacteria is (i.e. endogenous or exogenous), verification of which of these features  
525 are in fact caused by microbial bioerosion is more urgent. Our results showed that Wedl  
526 tunnelling, Wedl 2, and lamellate MFD are not reliable indicators of decomposition because  
527 similar features appear on freshly burnt bones, and thus can be caused by other factors, such  
528 as burning. Budded MFD was the only feature that showed a statistically significant increase  
529 in bone areas affected on both the unburnt and burnt groups. However, burning considerably  
530 reduced the visibility of this feature. Features labelled here as similar to 'cyanobacterial  
531 tunnelling' were in fact probably Volkmann's canals, which survived cremation on all bones.  
532 Hairline cracks did not appear to be informative on decay. Although BSEM is a useful tool in

533 bioerosion studies in unburnt bones, it cannot be used on burnt bones. In summary, it can be  
534 argued that microbial bioerosion features are not accurate proxies for the body's pre-burning  
535 condition and caution should be practised when identifying these in bones in both forensic  
536 and archaeological contexts.

## 537 Acknowledgements

538 The study was supported by the Meyerstein Foundation, School of Archaeology, University  
539 of Oxford. We would like to thank Prof. Robert Hedges for his insights into the study and Dr  
540 Victoria Smith for her help on the electron microprobe. We would also like to thank Mr  
541 Kevin Lemagnen for his help and support while developing the data labelling application. We  
542 thank the anonymous reviewers for their careful reading, valuable comments, and  
543 improvements made to the paper.

## 544 Funding

545

546 This work was supported by the Meyerstein Foundation, School of Archaeology, University  
547 of Oxford.

## 548 References

549

550 Absolonova, K., Veleminsky, P., Dobisikova, M., Beran, M., and Zocova, J. (2013). Histological  
551 estimation of age at death from the compact bone of burned and unburned human ribs.  
552 *Journal of Forensic Sciences*, 58, S135-S145.

553 Baby, R. S. (1954). Hopewell cremation practices. *Papers in Archaeology*. Ohio Historical  
554 Society, 1–7.

555 Bell, L. S. (2012a). Histotaphonomy. In C. Crowder and S. Stout (Eds.), *Bone Histology: An*  
556 *Anthropological Perspective* (pp. 241–251). Boca Raton, FL: Taylor and Francis.

557 Bell, L. S. (2012b). Identifying postmortem microstructural change to skeletal and dental  
558 tissues using backscattered electron imaging. In Lynne S. Bell (Ed.), *Forensic Microscopy for*  
559 *Skeletal Tissues* (pp. 173–190). Humana Press.

560 Bell, L. S., Boyde, A., Jones, S. J., and Bell, L. S. (1991). Diagenetic alteration to teeth in situ  
561 illustrated by backscattered electron imaging, 13, 173–183.

562 Bell, L. S., Skinner, M. F., and Jones, S. J. (1996). The speed of post mortem change to the  
563 human skeleton and its taphonomic significance. *Forensic Science International*, 82(2), 129–  
564 140.

565 Binford, L. R. (1963). An analysis of cremations from three Michigan sites. *Wisconsin*  
566 *Archaeologist*, 44, 98–110.

567 Boaks, A., Siwek, D., and Mortazavi, F. (2014). The temporal degradation of bone collagen: A  
568 histochemical approach. *Forensic Science International*, 240, 104-110.

569 Bonney, H., Colston, B., and Goodman, A. (2011). Regional variation in the mechanical  
570 properties of cortical bone from the porcine femur. *Medical Engineering and Physics*, 33(4),  
571 513-520.

572 Bontrager, A. B., and Nawrocki, S. P. (2008). Cremains from the Fox Hollow Farm serial  
573 homicide site. In: Schmidt C. W., Symes S. A., editors. *The Analysis of Burned Human*  
574 *Remains*. London: Academic Press; 2008, 211–226.

575 Booth, T. J., and Madgwick, R. (2016). New evidence for diverse secondary burial practices in  
576 Iron Age Britain: A histological case study. *Journal of Archaeological Science*, 67, 14– 24.

577 Boskey, A. L., and Coleman, R. (2010). Critical reviews in oral biology and medicine: Aging  
578 and bone. *Journal of Dental Research*, 89(12), 1333–1348.  
579 <https://doi.org/10.1177/0022034510377791>

580 Bradtmiller, B., and Buikstra, J. E. (1984). Effects of burning on human bone microstructure:  
581 a preliminary study. *Journal of Forensic Sciences*, 29(2), 535–540.

582 Brönnimann, D., Portmann, C., Pichler, S. L., Booth, T. J., Röder, B., Vach, W., ... Rentzel, P.  
583 (2018). Contextualising the dead – Combining geoarchaeology and osteoanthropology in a  
584 new multi-focus approach in bone histotaphonomy. *Journal of Archaeological Science*,  
585 98(August), 45–58.

586 Buikstra, J. E., and Swegle, M. (1989). Bone modification due to burning: experimental  
587 evidence. In Bonnicksen, R. and Sorg, M. (Eds.), *Bone Modification*, College Station, TX: The  
588 Centre for the Study of the First Americans, 247–258.

589 Cambra-Moo, O., Barroso Bermejo, R., García Gil, O., Bueno Ramírez, P., Rascón Pérez, J.,  
590 González Martín, A., ... Rietveld, H. M. (2017). The effect of soft tissue on temperature  
591 estimation from burnt bone using Fourier Transform Infrared Spectroscopy. *Journal of*  
592 *Forensic Sciences*, 35(1), 1–8.

593 Carroll, E. L., and Kirsty E. Squires. "Burning by Numbers: A Pilot Study Using Quantitative  
594 Petrography in the Analysis of Heat-induced Alteration in Burned Bone." *International*  
595 *Journal of Osteoarchaeology* 30.5 (2020): 691-99. Web.

596 Castillo, F., Ubelaker, D. H., Acosta, J. A., de la Rosa, R. J., and Garcia, I. G. (2013). Effect of  
597 temperature on bone tissue: Histological changes. *Journal of Forensic Sciences*, 58(3), 578–  
598 582. <https://doi.org/10.1111/1556-4029.12093>

599 Cattaneo, C., DiMartino, S., Scali, S., Craig, O. E., Grandi, M., and Sokol, R. J. (1999).  
600 Determining the human origin of fragments of burnt bone: A comparative study of  
601 histological, immunological and DNA techniques. *Forensic Science International*, 102(2–3),  
602 181–191.

603 Child, A. (1995). Towards and Understanding of the Microbial Decomposition of  
604 Archaeological Bone in the Burial Environment. *Journal of Archaeological Science*, 22(2),  
605 165-174.

606 Cooney, G., Quinn, C., P., Kuijt, Ian (2014). *Transformation by fire*. Tucson : University of  
607 Arizona Press.

608 Collins, M. J., Nielsen–Marsh, C. M., Hiller, J., Smith, C. I., Roberts, J. P., Prigodich, R. V., ...  
609 Turner–Walker, G. (2002). The survival of organic matter in bone: a review. *Archaeometry*.  
610 44(3), 383-394.

611 Daniel, J. C., and Chin, K. (2010). The role of bacterially mediated precipitation in the  
612 permineralization of bone. *PALAIOS. SEPM (Society for Sedimentary Geology)*. 25(7/8), 507-  
613 516.

614 Dowd, M. A. (2008). The use of caves for funerary and ritual practices in Neolithic Ireland.  
615 *Antiquity*, 82, 305–317.

616 Etxeberria, F. (1994). Aspectos macroscópicos del hueso sometido al fuego: revisión de las  
617 cremaciones descritas en el País Vasco desde la arqueología. *Munibe*, 46, 111–116.

618 Fairgrieve, S. I. (2008). *Forensic Cremation Recovery and Analysis*. Boca Raton, FL: CRC Press.

619 Farmer, A. (1995). Soil chemistry change in a lowland english deciduous Woodland 1974–  
620 1991. *Water, Air, and Soil Pollution*. 85(2), 677-682.

621 Farmer, A. (1995). Soil chemistry change in a lowland english deciduous Woodland 1974–  
622 1991 [Article]. In *Water, Air, and Soil Pollution (Vol. 85, Issue 2, pp. 677–682)*. Kluwer  
623 Academic Publishers. <https://doi.org/10.1007/BF00476907>

624 Feng, L., and Jasiuk, I. (2011). Multi-scale characterization of swine femoral cortical bone.  
625 *Journal of Biomechanics*, 44(2), 313-320.

626 Fernández-Jalvo, Y., Andrews, P., Pesquero, D., Smith, C., Marín-monfort, D., Sánchez, B., ...  
627 Alonso, A. (2010). Early bone diagenesis in temperate environments Part I : Surface features  
628 and histology. *Palaeogeography, Palaeoclimatology, Palaeoecology*, 288(1–4), 62–81.

629 Forbes, S. L., Stuart, B. H., and Dent, B. B. (2005). The effect of the method of burial on  
630 adipocere formation. *Forensic Science International*, 154(1), 44-52.

631 Garland, A. N. (1987) A histological study of archaeological bone decomposition.  
632 Boddington, A., Garland, A. N., Janaway, R. C. (Eds.), *Death, Decay, and Reconstruction:  
633 Approaches to Archaeology and Forensic Science*. Manchester University Press, Manchester,  
634 109– 126.

635 Garrido-Varas, C., and Intriago-Leiva, M. (2015). The interpretation and reconstruction of  
636 the post-mortem events in a case of scattered burned remains in Chile. In T. Thompson  
637 (Ed.), *The Archaeology of Cremation: burned human remains in funerary studies*.  
638 Havertown: Oxbow Books, 227-242.

639 Gonçalves, D., Thompson, T. J. U., and Cunha, E. (2011). Implications of heat-induced  
640 changes in bone on the interpretation of funerary behaviour and practice. *Journal of*  
641 *Archaeological Science*, 38(6), 1308–1313.

642 Grévin, G., Baud, C., and Susini, A. (1991). Etude anthropologique et paléopathologique d'  
643 un adulte inhumé puis incinéré provenant du site de Pincevent ( Seine-et-Marne ), *Bulletins*  
644 *et Mémoires de la Société d'Anthropologie de Paris* 2(3-4), 77–87.

645 Grine, F. E., Bromage, T. G., Daegling, D. J., Burr, D. B., and Brain, C. K. (2015). Microbial  
646 osteolysis in an Early Pleistocene hominin ( *Paranthropus robustus* ) from Swartkrans , South  
647 Africa. *Journal of Human Evolution*, 85, 126–135.

648 Hackett C.J. (1981). Microscopical Focal Destruction (Tunnels) in Exhumed Human Bones.  
649 *Medicine, Science and the Law*, 21(4), 243–265.

650 Hedges, R. E. M., and Millard, A. R. (1995). Bones and Groundwater: Towards the Modelling  
651 of Diagenetic Processes. *Journal of Archaeological Science* 22/ 2, 155–164.  
652 <https://doi.org/10.1006/jasc.1995.0017>

653 Hedges, R.E.M., Millard, A.R., Pike, A.W.G., (1995). Measurements and relationships of  
654 diagenetic alteration of bone from three archaeological sites. *Journal of Archaeological*  
655 *Science*, 22, 201-209. <https://doi.org/10.1006/jasc.1995.0022>

656 Herrmann, B. (1976). Neuere Ergebnisse zur Beurteilung menschlicher Brandknochen. *Z.*  
657 *Rechtsmedizin*, 17, 191–200.

658 Herrmann, B. (1977). On histological investigations of cremated human remains. *Journal of*  
659 *Human Evolution*, .6(2), 101-103.

660 Holden, J., Phakey, P., and Clement, J. (1995). Scanning electron microscope observations of  
661 heat-treated human bone. *Forensic Science International*, 74(1-2), 29-45.

662 Holden, J. L., Clement, J. G., and Phakey, P. P. (1995). Age and temperature related changes  
663 to the ultrastructure and composition of human bone mineral. *Journal of Bone and Mineral*  
664 *Research*, 10(9), 1400-1409.

665 Hollund, H. I., Jans, M. M. E., Collins, M. J., Kars, H., Joosten, I., and Kars, S. M. (2012). What  
666 Happened Here? Bone Histology as a Tool in Decoding the Postmortem Histories of  
667 Archaeological Bone from Castricum, The Netherlands. *International Journal of*  
668 *Osteoarchaeology*, 22(5), 537-548.

669 Hollund, Hege I, Jans, M. M. E., and Kars, H. (2014). How are teeth better than bone? An  
670 investigation of dental tissue diagenesis and state of preservation at a histological scale  
671 (with photo catalogue). *Internet Archaeology* 36.

672 Huisman, D.J., Raemaekers, D.C.M., Jongmans, A.G. (2009). Investigating Early Neolithic land  
673 use in Swifterbant (NL) using micromorphological techniques. *Catena* 78(3), 185e197.

674 Huisman, H., Ismail-Meyer, K., Sageidet, B. M., and Joosten, I. (2017). Micromorphological  
675 indicators for degradation processes in archaeological bone from temperate European  
676 wetland sites. *Journal of Archaeological Science*, 85, 13-29.

677 Hummel, S., and Schutkowski, H. (1986). Bedeutungen für die Leichenbranddiagnose. Mit 4  
678 Abbildungen und 1 Tabelle im Text. *Zeitschrift für Morphologie und Anthropologie*, 77(1), 1-  
679 9.

680 Imaizumi, K., Taniguchi, K., and Ogawa, Y. (2014). DNA survival and physical and histological  
681 properties of heat-induced alterations in burnt bones. *International Journal of Legal  
682 Medicine*, 128(3), 439-446.

683 Jans, M. M.E., Nielsen-Marsh, C. M., Smith, C. I., Collins, M. J., and Kars, H. (2004).  
684 Characterisation of microbial attack on archaeological bone. *Journal of Archaeological  
685 Science*, 31(1), 87–95.

686 Jans, M. M. E, Kars, H., Nielsen-Marsh, C. M., Smith, C. I., Nord, A. G., Arthur, P., and Earl, N.  
687 (2002). in *Situ Preservation of Archaeological Bone: a Histological Study Within a  
688 Multidisciplinary Approach*. *Archaeometry*, 44, 343–352.

689 Jans, M. M. E. (2005). *Histological Characterisation of Diagenetic Alteration of  
690 Archaeological Bone*. (Unpublished doctoral dissertation) Amsterdam: Institute for Geo and  
691 Bioarchaeology.

692 Jans, M. M. E. (2008). Microbial bioerosion of bone - a review. In Wisshak, M. and Tapanila,  
693 L. (Eds.), *Current Developments in Bioerosion*. Berlin, Heidelberg: Springer, 397-493.

694 Jans, M. M E. (2013). Microscopic destruction of bone. In J. T. Pokines and S. A. Symes (Eds.),  
695 *Manual of Forensic Taphonomy*, CRC Press, Taylor and Francis group, 19-35.

696 Kendall, C., Marie, A., Eriksen, H., Collins, M. J., Turner-Walker, G., and Kontopoulos, I.  
697 (2018). Diagenesis of archaeological bone and tooth. *Palaeogeography, Palaeoclimatology,  
698 Palaeoecology*, 491(November 2017), 21–37.

699 Kontopoulos, I. (2019). Bone diagenesis in a Mycenaean secondary burial (Kastrouli,  
700 Greece), *Archaeological and Anthropological Sciences*, 11, 5213–5230.

701 Kontopoulos, I., Nystrom, P., and White, L. (2016). Experimental taphonomy : post-mortem  
702 microstructural modifications in *sus scrofa domestica* bone. *Forensic Science International*,  
703 266(April 2019), 320–328.

704 Lemmers, S. A. M., Gonçalves, Cunha, E., D., Vassalo, A., R., and Appleby, J. (2020). Burned  
705 Fleshed or Dry ? The Potential of Bioerosion to Determine the Pre-Burning Condition of  
706 Human Remains. *Journal of Archaeological Method and Theory*.

707 Lynn, K. S., and Fairgrieve, S. I. (2009). Microscopic Indicators of Axe and Hatchet Trauma in  
708 Fleshed and Defleshed Mammalian Long Bones. *Journal of Forensic Sciences*, 54(4), 793–  
709 797.

710 Millard, A. (1993). Diagenesis of archaeological bone: the case of uranium uptake.  
711 (Unpublished doctoral thesis) University of Oxford: Research Laboratory for Archaeology  
712 and the History of Art.

713 Millard, A. R. (2001). Deterioration of Bone. In D. R. Brothwell and A. M. Pollard (Eds.),  
714 Handbook of Archaeological Sciences. Chichester ; New York : J. Wiley, 637-647.

715 Morales, N. S., Catella, L., Oliva, F., Sarmiento, P. L., and Barrientos, G. (2018). Journal of  
716 Archaeological Science: Reports. A SEM-based assessment of bioerosion in Late Holocene  
717 faunal bone assemblages from the southern Pampas of Argentina. Journal of Archaeological  
718 Science: Reports, 18, 782–791.

719 Nelson, R. (1992). A Microscopic Comparison of Fresh and Burned Bone. Journal of Forensic  
720 Sciences, 37(4), 1055–1060.

721 Nicholson, R. A. (1993). A morphological investigation of burnt animal bone and an  
722 evaluation of its utility in archaeology. Journal of Archaeological Science, 20(4), 411- 428.

723 Nielsen-Marsh, C. M., and Hedges, R. E. . (2002). Patterns of Diagenesis in Bone I: The Effects  
724 of Site Environments. Journal of Archaeological Science, 27(12), 1139–1150.

725 Nielsen-Marsh, C. M., Smith, C. I., Jans, M. M. E., Nord, A., Kars, H., and Collins, M. J. (2007).  
726 Bone diagenesis in the European Holocene II : taphonomic and environmental  
727 considerations. Journal of Archaeological Science, 34(9), 1523-1531.

728 Pearce, A. I., Richards, R. G., Milz, S., Schneider, E., and Pearce, S. G. (2007). Animal models  
729 for implant biomaterial research in bone: A review. European Cells and Materials, 13(0), 1–  
730 10. <https://doi.org/10.22203/eCM.v013a01>

731 Pechal, J. L., Tawni L Crippen, Aaron M Tarone, Andrew J Lewis, Jeffery K Tomberlin, and M  
732 Eric Benbow. (2013). Microbial community functional change during vertebrate carrion  
733 decomposition. PLoS ONE. 8(11), e79035.

734 Pesquero, M. D., Bell, L. S., Fernández-jalvo, Y., Pesquero, M. D., Bell, L. S., and Fernández-  
735 jalvo, Y. (2018). Skeletal modification by microorganisms and their environments. Historical  
736 Biology, 2963, 1–12. <https://doi.org/10.1080/08912963.2017.1371713>

737 Piepenbrink, H. (1986). Two examples of biogenous dead bone decomposition and their  
738 consequences for taphonomic interpretation. Journal of Archaeological Science, 13(5), 417-  
739 430.

740 Piepenbrink, H., and Schutkowski, H. (1987). Decomposition of skeletal remains in desert dry  
741 soil A roentgenological study. Human Evolution, 2(6), 481–491.

742 Quatrehomme, G., Bolla, M., Muller, M., Rocca, J., Grévin, G., Bilet, P., and Ollier, A. (1998).  
743 Experimental Single Controlled Study of Burned Bones: Contribution of Scanning Electron  
744 Microscopy. Journal of Forensic Sciences, 43(2), 417–422.

745 Roux, G. A. D. T. (1887). Contribution à l'étude clinique et thérapeutique des taenias de  
746 l'homme. (Unpublished doctoral thesis) University of Lyon, Lyon, France.

747 Spennemann, D. H. R., Colley, S. M. (1989). Fire in a Pit: the effects of burning on faunal  
748 remains. *Archaeozoologia*, 3, 51–64.

749 Squires, K. E., Thompson, T. J. U., Islam, M., and Chamberlain, A. (2011). The application of  
750 histomorphometry and Fourier Transform Infrared Spectroscopy to the analysis of early  
751 Anglo-Saxon burned bone. *Journal of Archaeological Science*, 38(9), 2399–2409.

752 Symes, A., S., Dirkmaat, D. C., Ousley, S., Chapman, E., Cabo, L. (2012) Recovery and  
753 Interpretation of Burned Human Remains. NIJ Report. National Institute of Justice Available  
754 at <https://www.ncjrs.gov/pdffiles1/nij/grants/237966.pdf> (20/04/2016).

755 Taylor, M. E., Morecroft, M. D., and Oliver, H. R. (2011). *The Physical Environment*. Wytham  
756 Woods. Oxford University Press.

757 Thompson, T. J. U., and Inglis, J. (2009). Differentiation of serrated and non-serrated blades  
758 from stab marks in bone. *International Journal of Legal Medicine*, 123(2), 129–135.

759 Tjellén, A. K. E., Kristiansen, S. M., Birkedal, H., and Jans, M. M. E. (2018). The pattern of  
760 human bone dissolution—A histological study of Iron Age warriors from a Danish wetland  
761 site. *International Journal of Osteoarchaeology*, 28(4), 407–418.

762 Trueman, C. N., and Martill, D. M. (2002). The long-term survival of bone: the role of  
763 bioerosion. *Archaeometry*. 44(3), 371-382.

764 Turner, B., and Wiltshire, P. (1999). Experimental validation of forensic evidence : a study of  
765 the decomposition of buried pigs in a heavy clay soil, *Forensic Science International* 101,  
766 113–122.

767 Turner-Walker, G. (2012). Early bioerosion in skeletal tissues : Persistence through deep  
768 time Early bioerosion in skeletal tissues: persistence through deep time, *Neues Jahrbuch für  
769 Geologie und Paläontologie - Abhandlungen* 265(2), 165-183.

770 Turner-Walker, G. (2014). The Chemical and Microbial Degradation of Bones and Teeth. In:  
771 Pinhasi, R. and Mays, S. (Eds.) *Advances in Human Palaeopathology*. John Wiley and Sons, 3-  
772 29.

773 Turner-Walker, G. (2019). Light at the end of the tunnels ? The origins of microbial  
774 bioerosion in mineralised collagen. *Palaeogeography, Palaeoclimatology, Palaeoecology*,  
775 529, 24–38.

776 Turner-Walker, G. and Syversen, U. (2002). Quantifying histological changes in  
777 archaeological bones using BSE-SEM image analysis. *Archaeometry*, 44(3), 461-468.

778 Turner-Walker, G. and Jans, M. (2008). Reconstructing taphonomic histories using  
779 histological analysis. *Palaeogeography, Palaeoclimatology, Palaeoecology*, 266(3), 227-235.

780 Turner-Walker, G. and Peacock, E.E. (2008). Preliminary results of bone diagenesis in  
781 Scandinavian bogs. *Palaeogeography, Palaeoclimatology, Palaeoecology*, 266(3-4), 151-159.

782 Ubelaker, D. H. (2009). The forensic evaluation of burned skeletal remains: A synthesis.  
783 *Forensic Science International*, 183(1–3), 1–5.

- 784 Upton, R. N., A. Checinska Sielaff, K. S. Hofmockel, X. Xu, H. W. Polley, and B. J. Wilsey. 2019.  
785 Soil depth and grassland origin cooperatively shape microbial community cooccurrence and  
786 function. *Ecosphere* 11(1):e02973.
- 787 Van Vark, G. N. (1970). *Some Statistical Procedures for the Investigation of Prehistoric*  
788 *Human Skeletal Material*. Groningen: Rijksuniversiteit te Groningen.
- 789 Waterman, D. M. (1978) The Excavation of a Court Cairn at Tully, Co. Fermanagh. *Ulster*  
790 *Journal of Archaeology* 41, 3–14.
- 791 Wedl, C. (1864). Über einen im Zahnbein und Knochen keimenden Pilz. *Sitzungsberichte Der*  
792 *Kaiserlichen Akademie Der Wissenschaften Zu Wien, Mathematisch- Naturwissenschaftliche*  
793 *Classe*, 50(1), 171–193.
- 794 Wells, C. (1978). Notes on Cremated Bones from Tully Court Cairn. *Ulster Journal of*  
795 *Archaeology*, 41, 13–14.
- 796 White, L., and Booth, T. J. (2014). The origin of bacteria responsible for bioerosion to the  
797 internal bone microstructure: Results from experimentally-deposited pig carcasses. *Forensic*  
798 *Science International*, 239, 92–102.
- 799 Whyte, T. (2001). Distinguishing remains of human cremations from burned animal bones.  
800 *Journal of Field Archaeology*, 28, 437–448.
- 801 Wilson, A. S., Janaway, R. C., Holland, A. D., Dodson, H. I., Baran, E., Pollard, A. M., Desmond,  
802 T. J. (2007). Modelling the buried human body environment in upland climes using three  
803 contrasting field sites. *Forensic Science International*, 169, 6–18.
- 804 Yoshino, M., Kimijima, T., Miyasaka, S., Sato, H., and Seta, S. (1991). Microscopical study on  
805 estimation of time since death in skeletal remains. *Forensic Science International*, 49(2),  
806 143-158. [https://doi.org/10.1016/0379-0738\(91\)90074-S](https://doi.org/10.1016/0379-0738(91)90074-S).

# Assessing the reliability of microbial bioerosion features in burnt bones: a novel approach using feature-labelling in histotaphonomical analysis

Végh, Emese I.

2021-03-22

Attribution-NonCommercial-NoDerivatives 4.0 International

---

Vegh E, Czermak A, Marquez-Grant N, Schulting R. (2021) Assessing the reliability of microbial bioerosion features in burnt bones: a novel approach using feature-labelling in histotaphonomical analysis. *Journal of Archaeological Science: Reports*, Volume 37, June 2021, Article number 102906

<https://doi.org/10.1016/j.jasrep.2021.102906>

*Downloaded from CERES Research Repository, Cranfield University*